Software for atmospheric correction of space IR measurements of the underlying surface temperature

S.V. Afonin, V.V. Belov, and D.V. Solomatov

Institute of Atmospheric Optics,
Siberian Branch of the Russian Academy of Sciences, Tomsk

Received December 5, 2005

Software for atmospheric correction of space IR measurements elaborated at the Institute of Atmospheric Optics SB RAS is described. The software is intended for two types of application: simulation of space measurements with the use of different satellite-borne and aircraft-borne sensors, as well as atmospheric correction of real-time space IR measurements of the underlying surface temperature (UST) with accounting for key distorting factors based on *a priori* data on optical-meteorological state of atmosphere and geometry of observations. The MODIS topical satellite data used as the *a priori* information in the atmospheric correction are concisely described. The structure of the software input data, general scheme, and illustrations of its operation are presented.

Introduction

By now, a considerable amount of information concerning different problems of atmospheric correction of underlying surface temperature remote measurements, as well as practical results of such a correction are described in scientific literature.[1,2] The ATCOR program models have been worked out for the well-known commercial software products ERDAS and ENVI intended for the satellite data processing. Standard algorithms of atmospheric correction in 0.47–2.13-μm channels have been elaborated for one of the last spectroradiometers MODIS of a moderate spatial resolution.

However, in a number of cases the atmospheric correction is carried out in a simplified way or with insufficient (for solution of a topical problem) precision, if at all. Such cases usually occur when large amounts of high-accuracy *a priori* information are required for atmospheric correction. Also, situations are possible when it is necessary to adapt the means intended for global atmospheric correction to local conditions. Hence, the creation of effective program means for atmospheric correction fully accounting for distorting factors with a required degree of accuracy is the issue of the day.

In this paper, the methodical, information, and algorithmic foundations for the software being under development at the Institute of Atmospheric Optics SB RAS are briefly described. The software is intended for two types of application: simulation of space measurements with the use of different sensors, as well as atmospheric correction of real-time space IR measurements of the underlying surface temperature (UST) with accounting for key distorting factors based on *a priori* data on optical-meteorological state of atmosphere and the underlying surface.

1. Mathematical and physical basis for atmospheric correction of space IR measurements of the underlying surface temperature

The intensity J_λ of thermal radiation upward flow, measured in the IR-channel, can be written as

$$J_\lambda = B_\lambda(T_R), \quad J_\lambda = J_{srf} + J_{atm} + J_{rfl} + J_{sct},$$

$$J_{srf} = \int \varphi_\lambda \varepsilon_\lambda^0 B_\lambda(T_S) P_\lambda \, d\lambda,$$

$$J_{atm} = \int \varphi_\lambda f_\lambda^{atm}\{\theta, T(h), \tau_\lambda(h)\} \, d\lambda,$$

$$J_{rfl} = \int \varphi_\lambda A_\lambda P_\lambda f_\lambda^{rfl}\{\theta, met, ext, sct\} \, d\lambda,$$

$$J_{sct} = \int \varphi_\lambda f_\lambda^{sct}\{\theta, met, ext, sct\} \, d\lambda,$$

where $B_\lambda(T)$ is the Planck function; φ_λ is the relative spectral characteristic of the IR channel (integration with respect to the wavelength λ is fulfilled in the spectral range of setting the φ_λ function); T_R is the radiation temperature equivalent to J_λ; T_S is the reconstructed UST; ε_λ^0 is the emissivity of the underlying surface (0–1); $A_\lambda = (1 - \varepsilon_\lambda^0)$ is the underlying surface albedo; $P_\lambda = \exp\{-\tau_\lambda(\theta)\}$ is the transmittance of atmosphere; τ_λ is the optical depth of atmosphere; θ is the slope angle of the device axis; J_{srf} is the contribution of atmosphere-attenuated thermal radiation of the surface; J_{atm} is the contribution of the atmospheric thermal radiation; J_{rfl} is the contribution of surface-reflected incident flux of thermal radiation; J_{sct} is the contribution of atmosphere-scattered flux of thermal radiation; (met) are the meteorological atmospheric parameters; (ext), (sct) are the extinction and scattering characteristics of the atmospheric aerosol.

0235-6880/06/01 62-07 $02.00

In practice, to estimate errors in remote UST measurements, the temperature correction $\Delta T_R = T_S - T_R$ is often used, which can be conventionally conceived of as a sum of two terms: $\Delta T_R = \Delta T_E + \Delta T_a$ determined by radiation (reflection) characteristics of the underlying surface and distorting properties of atmosphere. The atmospheric factor ΔT_a is determined from the conditions $\varepsilon_\lambda^0 = 1$, $A_\lambda = 0$, $J_{rfl} = 0$, i.e. UST reconstruction and $\Delta T_a = T_{S,a} - T_R$ calculation are carried out for an absolutely black surface. The contribution of the first factor can be easily estimated as $\Delta T_E = \Delta T_R - \Delta T_a$.

1.1. Distortions in remote UST measurements

Table 1 presents some estimates of distorting influence of atmosphere on IR measurements of the UST in the 10.4–12.6 μm channel of the AGROS airborne radiometer.[3] Standard meteorological models of atmosphere[4] were used in calculations: 1) tropics (the surface temperature $T_S = 300$ K, the moisture content $W = 4.19$ g/cm^2), 2) mid-latitude summer ($T_S = 294$ K, $W = 2.98$ g/cm^2), 3) mid-latitude winter ($T_S = 272$ K, $W = 0.86$ g/cm^2), and 4) arctic summer ($T_S = 287$ K, $W = 2.12$ g/cm^2).

Key distorting factors for the underlying surface IR-radiation in the spectral ranges 3.5–4 and 8–13 μm in the condition of cloudless atmosphere are the following:

– selective molecular absorption,
– continual absorption,
– aerosol absorption and scattering.

Table 2 presents data from Ref. 1 on the magnitude of atmospheric distortions of UST measurements in the satellite radiometer AVHRR/NOAA channels for four above-mentioned atmospheric models.

Table 1. Errors (°C) of UST measurements in the 10.4–12.6 μm IR channel

H, km	Integral water content of atmosphere W, g/cm^2							
	4.19		2.98		2.12		0.86	
	Slope angle of the device axis θ, deg.							
	0	35	0	35	0	35	0	35
Effect of the molecular atmospheric component								
0.5	0.34	0.39	0.20	0.22	0.16	0.18	0.07	0.08
1.0	0.93	1.06	0.52	0.59	0.42	0.48	0.15	0.16
1.5	1.71	1.96	0.93	1.06	0.77	0.88	0.26	0.30
2.0	2.45	2.80	1.28	1.47	1.08	1.23	0.37	0.41
2.5	3.11	3.55	1.65	1.89	1.40	1.61	0.49	0.55
3.0	3.53	4.04	1.95	2.24	1.67	1.91	0.58	0.66
4.0	4.13	4.71	2.47	2.82	2.13	2.44	0.80	0.90
5.0	4.57	5.21	2.84	3.24	2.48	2.83	1.00	1.13
100	7.73	8.80	6.16	6.98	5.49	6.22	3.86	4.33
Effect of aerosol (MRV = 5 km)								
0.5	0.07	0.10	0.09	0.13	0.10	0.14	0.10	0.13
2.5	0.23	0.28	0.26	0.34	0.30	0.39	0.27	0.38
5.0	0.26	0.31	0.28	0.36	0.33	0.43	0.30	0.40
100	0.28	0.33	0.29	0.38	0.34	0.43	0.30	0.40
Effect of the underlying surface emissivity ($\varepsilon_\lambda^0 = 0.95$)								
0.5	1.06	1.02	1.48	1.45	1.88	1.85	2.24	2.22
2.5	0.78	0.71	1.23	1.15	1.67	1.6	2.13	2.10
5.0	0.75	0.67	1.19	1.11	1.61	1.55	2.10	2.07
100	0.72	0.64	1.15	1.07	1.57	1.49	2.06	2.02

N o t e . H is the flight altitude; MRV is the meteorological range of visibility.

Table 2. The radiation temperature correction, °C

Model No.	Channel, μm			
	3.55–3.95	8.30–9.30	10.5–11.5	11.5–12.5
Selective molecular absorption				
1	2.01	3.56	1.30	2.34
2	1.49	2.82	0.87	1.60
3	0.72	1.46	0.24	0.47
4	1.32	2.48	0.69	1.29
Continual absorption				
1	0.62	2.72	3.81	4.87
2	0.44	1.37	1.81	2.35
3	0.22	0.26	0.27	0.35
4	0.44	1.10	1.42	1.86

Thus, the atmospheric correction of the space-measured underlying surface temperature T_R includes the following steps:

1) calculation of J_{atm}, J_{rfl}, J_{sct}, and P_λ using *a priori* data on optical-meteorological state of atmosphere, the underlying surface emissivity, and the geometry of observations;

2) calculation of $J_{srf} = J_\lambda - (J_{atm} + J_{rfl} + J_{sct})$;

3) determination of the UST value T_S using pre-calculated tables for T_S dependence of J_{srf}.

1.2. Atmospheric distortion of thermal contrasts

When studying thermal contrasts on the underlying surface (US), their distortions due to atmosphere effect are observable. Let $\Delta T_{12} = T_1 - T_2$ be the thermal contrast on the underlying surface, where T_1 and T_2 are temperatures of two US areas. Assume similar optical-geometrical observation conditions for the above areas. Some simple calculations show that the thermal contrast, observable during space measurements, can be written as $\Delta T_c = K_c \Delta T_{12}$, where the contrast coefficient K_c is proportional to the atmospheric transmittance function P_λ.

Table 3 presents the contrast coefficients K_c for the 10.4–12.6 μm channels of the AGROS device depending on the weather and the geometry of observations. The data show a significant decrease (from 0.95 to 0.5) in K_c magnitude with increasing flight altitude and water content in atmosphere.

2. Data of MODIS Atmosphere (Land) Products

2.1. A concise description of MODIS topical satellite data

Atmospheric correction of the satellite IR measurements of the UST is based on optical atmospheric models and *a priori* data on actual optical and meteorological conditions of atmosphere during space observations. According to Ref. 5, data from regional ground weather stations, as well as vertical radio-sounding data on the air temperature and humidity can be used as sources of *a priori* meteorological information. In addition, satellite measurement data, e.g. NOAA/ATOVS, EOS/MODIS, and, in particular, MODIS Atmosphere (Land) Products topical data can be used to enlarge spatial covering of observational areas by *a priori* data.

Topical MODIS Atmosphere Products (MODIS-AP) is the result of reconstruction of optical and meteorological atmospheric parameters from MODIS (Moderate Resolution Imaging Spectroradiometer) data (TERRA and AQUA satellites, http://modis.gsfc.nasa.gov/). The instrument measures in 36 spectral channels (0.405–14.385 μm) at 1000, 500, and 250-m spatial resolutions.

The MODIS-AP information can be Internet-ordered and ftp-transferred via network communications.

For atmospheric correction, three types of the key MODIS-AP data can be used: 1) aerosol characteristics (MOD04), 2) integral content of water vapor in atmosphere (MOD05), and 3) vertical profiles of geopotential, atmospheric temperature and moisture (MOD07). A brief description of these data is given in Table 4 (Ref. 6).

2.2. An example of the use of MODIS data in practice

For test calculations, vertical profiles of meteorological parameters, optical parameters of atmosphere, and underlying surface parameters were chosen with the following time and spatial characteristics:

September 22, 2004, 10:20 a.m. and 11:55 a.m.;
September 23, 2004, 07:05 p.m. and 08:45 p.m.;
coordinates: 66.913°N, 63.943°E.

Figure 1 and Table 5 show a comparison of the satellite meteorological data with test radiosensing atmospheric parameters. A good agreement between *a priori* MODIS-AP data and upper-air temperature measurements is seen from Fig. 1.

Table 3. The coefficient of thermal surface contrasts K_c from IR measurements by AGROS device

H, km	Integral water content in atmosphere W, g/cm^2							
	4.19		2.98		2.12		0.86	
	Slope angle of the device axis θ, deg.							
	0	35	0	35	0	35	0	35
0.5	0.798	0.766	0.856	0.834	0.904	0.890	0.954	0.948
1.0	0.706	0.662	0.788	0.754	0.860	0.838	0.934	0.924
1.5	0.646	0.596	0.746	0.706	0.832	0.806	0.920	0.910
2.0	0.604	0.548	0.716	0.676	0.812	0.782	0.910	0.898
2.5	0.580	0.522	0.700	0.656	0.798	0.768	0.904	0.890
3.0	0.564	0.508	0.690	0.646	0.790	0.756	0.898	0.884
4.0	0.552	0.494	0.680	0.634	0.778	0.746	0.892	0.878
5.0	0.548	0.490	0.676	0.628	0.774	0.740	0.890	0.874
100	0.530	0.468	0.652	0.600	0.744	0.706	0.860	0.840

Table 4. Brief description of MODIS data

Parameter	Data type		
	MOD04	MOD05	MOD07
Spatial resolution	10×10 km	1×1 km	5×5 km
Main parameters	aerosol type; aerosol optical depth (λ = 0.47, 0.55, and 0.66 μm); Angström index; mass concentration	integral water content	surface: *temperature*, *pressure*; vertical profiles: *geopotential*, *air temperature*, *dew-point temperature;* integral ozone content, integral water content
Granule size, MB	11	20	30

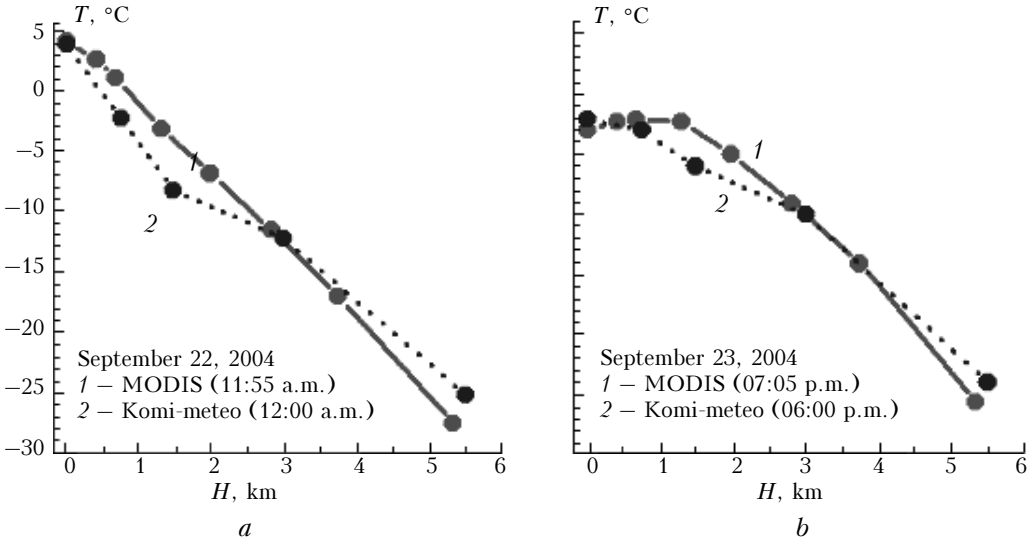

Fig. 1. Comparison of MODIS data with radio-sounding atmospheric parameters.

Table 5. Comparison of satellite and ground meteorological data at the surface level

Parameter	September 22, 2004		September 23, 2004	
	MODIS (11:55 a.m.)	Radio-sounder (12:00 a.m.)	MODIS (07:05 p.m.)	Radio-sounder (07:00 p.m.)
T of air, °C	4.4	4.1	−3.0	−2.9
T of surface, °C	6.2	6.0	−3.3	−3.5
Rel. air humidity, %	68.2	75	61.7	66.7

Calculation results

Based on satellite meteorological data on the state of atmosphere received at the time of aircraft measurements, relative contributions of radiation upward flow components were calculated for the AGROS IR channel:

– srf – thermal radiation of the underlying surface (for given ε_λ^0 and T_S);

– atm – thermal self-radiation of atmosphere and aerosol-scattered radiation (for given MRV);

– rfl – surface-reflected incident radiation (for given ε_λ^0).

Calculation parameters:

– MRV = 30 km (MOD04);

– surface emissivity $\varepsilon_\lambda^0 = 0.975$ (MOD11);

– T_S is given in Table 6;

– vertical profiles of meteorological parameters of atmosphere (MOD07 and MOD05) are given in Fig. 1; the mid-latitude summer meteomodel was also used;

– flight altitude H = 5 km, scanning angles θ = 0 and 35°.

Table 6. Relative contribution of radiation upward flow components

Weather condition	θ, deg.	Correction of UST, °C	Component contribution, %		
			srf	atm	rfl
September 22, 2004 (11:55 a.m.)	0	2.86	87.15	12.51	0.35
	35	3.09	85.32	14.35	0.34
September 23, 2004 (07:05 p.m.)	0	1.55	89.28	10.45	0.28
	35	1.61	87.85	11.88	0.27
Mid-latitude summer model	0	3.38	76.75	22.65	0.60
	35	3.71	73.37	26.06	0.57

It can be concluded from Table 6, that during the table-listed days, distorting effect of atmospheric processes (radiation, scattering, and absorption) at relatively low values of temperature, humidity, and aerosol content was only about 10–15%. However, accounting for the UST correction, a significant difference between the distorting atmospheric factors should be noted even for rather close in time observation moments. This once again proves the importance of real-time *a priori* data on the atmosphere state in reaching maximal precision in atmospheric correction of IR measurements.

In case of increased values of meteorological parameters (mid-latitude summer model) their distorting contribution can exceed 20%. Note, that the aerosol transparency of atmosphere was very high during the test measurements. However, distorting contribution of atmospheric processes (scattering and extinction) in the recorded signals will significantly rise with an increase of the aerosol content in atmosphere.

3. Software and general procedure of atmospheric correction of satellite IR measurements of UST

For atmospheric correction, the software packages, well-reputed in problems of simulating optical radiation transfer, e.g. LOWTRAN, MODTRAN, 6S etc., can be used as a basis. The LOWTRAN-7 was chosen for the first version of the software for atmospheric distortion calculations. The interface is written in C language (Fig. 2); the required operating systems are WINDOWS 98/2000/XP.

3.1. Input data

The program run begins with the input of files and command qualifiers through the program interface.

The list of input files:

- satellite measurements (image);
- image metadata describing its structure and specifications;
- relief (heights) of the underlying surface;
- spatial distribution of vertical profiles of air temperature and humidity (radiosensing data or MOD07 and MOD05 data);
- spatial distribution of aerosol optical characteristics (MOD04);
- spatial distribution of underlying surface characteristics, i.e., temperature and emissivity (MOD11);
- spectral characteristics of device channels (in case that the sensor is not described in the basic software).

The list of input parameters:

– geographical coordinates of ROI (Region of Interest);

– date and time of measurements;

– type of satellite/sensor and the list of the channel numbers used in calculations;

– orbit (flight) altitude;

– slope angle of the device axis;

– solar elevation angle and solar azimuth;

– sign of the type of *a priori* optical-meteorological data (AOMD):

a) 1, 2, ..., 6 for the number of the standard meteorological model from LOWTRAN-7,

b) 7 for radio-sounding data,

c) 8 for topical MODIS satellite data;

– file name of AOMD (for AOMD > 6);

– type of aerosol and MRV.

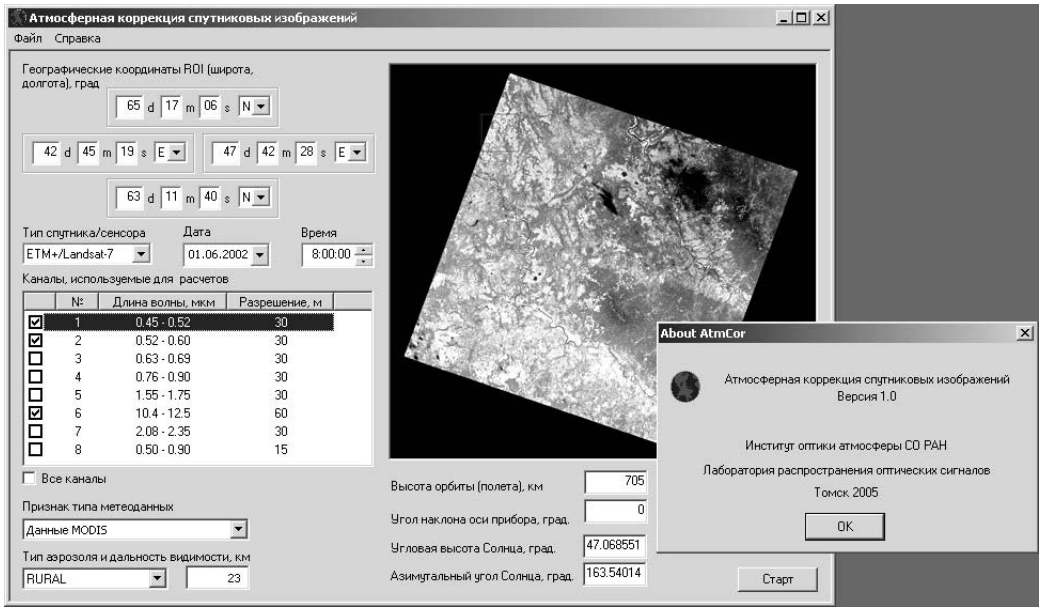

Fig. 2. An example of the program interface. The special window contains the image p177r015_7k20020601_z38_nn61.tif received in the 6th channel of the ETM+/Landsat-7 satellite system on June 1, 2002.

3.2. General scheme of operation

The user operation procedure includes the following steps:

1. Assignment of a spatial region of interest (ROI); filing satellite measurement data in a text or binary format.

2. Calibration of satellite data with the use of calibration data (from the metadata file), i.e., transformation of initial satellite data into radiation intensity values J_λ of $W/(m^2 \cdot sr \cdot \mu m)$ units.

3. A choice of MODIS files (MOD04, MOD05, MOD07, MOD11, see Fig. 3) maximally matched in time and location with satellite UST measurements. Figure 4 shows spatial distribution of MOD04 and MOD07 data chosen for the satellite image in Fig. 2.

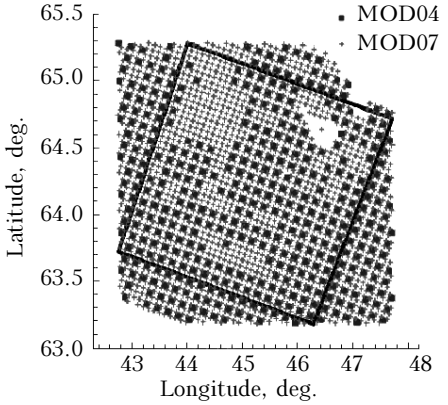

Fig. 4. Spatial resolution of MOD04 (418 points) and MOD07 (2036 points) data for the p177r015_7k20020601_z38_nn61.tif image.

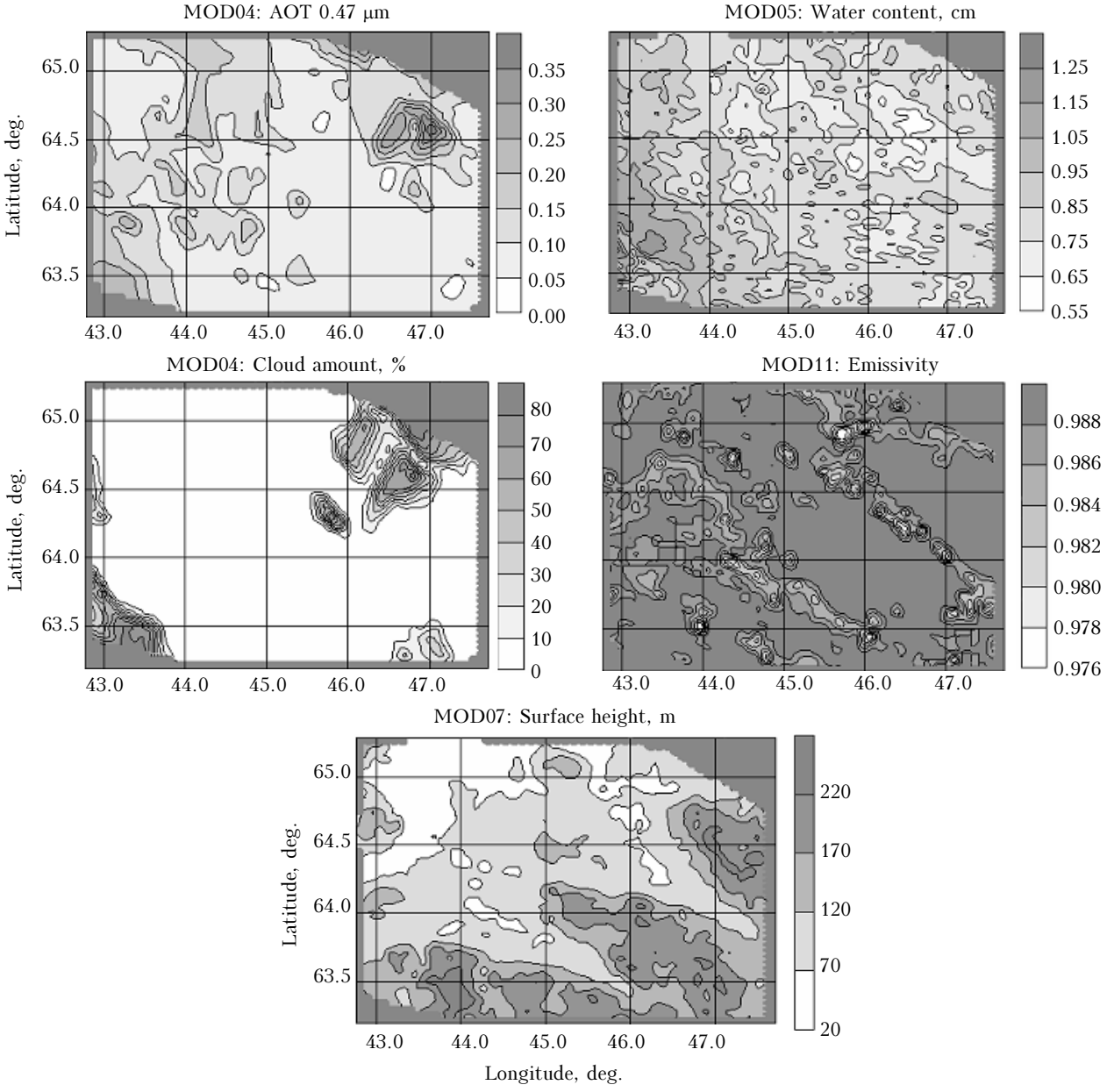

Fig. 3. Parameters of *a priori* MODIS Atmosphere (Land) Products data for the p177r015_7k20020601_z38_nn61.tif image.

4. Preliminary forming of consistent files with *a priori* MODIS data and their transformation from the HDF-EOS format into the text format using special programs (IDL/ENVI and/or C languages).

5. Setting the MOD04 file (aerosol data) with following going from measurements of aerosol optical depths to meteorological ranges of visibility and formation of the spatial distribution matrix according to the data snapshot.

6. Setting the MOD05, MOD07, and MOD11 files; and formation of the corresponding matrices of vertical profiles of air temperature and humidity, integral water content of atmosphere, underlying surface emissivity ε_λ^0 at λ = 11 and 12 μm.

7. Setting input files and parameters and calculating J_{atm}, J_{rfl}, J_{sct}, and P_λ interpolation arrays on the base of *a priori* data on the optical-meteorological state of atmosphere, the underlying surface emissivity (ε_λ^0), and the observation geometry. As an example, Table 7 presents J_{atm}, J_{rfl}, and P_λ statistics obtained on the basis of calculations for the ETM+/Landsat-7 6th channel using *a priori* MODIS data (neglecting aerosol).

8. Calculation of J_{atm}, J_{rfl}, J_{sct}, and P_λ for every pixel of the image on the basis of interpolation arrays with the use of data on the underlying surface relief.

Table 7

Parameter	Average	RMS deviation	Min	Max
J_{atm}	1.1722	0.1301	0.6289	1.5910
J_{rfl}	1.3100	0.1357	0.7134	1.6206
P_λ	0.8153	0.0168	0.7594	0.8865

Note. Profiles of meteorological parameters were taken from the 152-0835.m07 file (2036 profiles).

9. Calculation of $J_{srf} = J_\lambda - (J_{atm} + J_{rfl} + J_{sct})$ for every pixel with following calculation of T_S on the basis of the calculated dependence $J_{srf}(T_S)$. Finally, the matrix of UST values is formed for the ROI.

Conclusion

The first version of software for atmospheric correction of space IR measurements of the underlying surface temperature is built. The software allows both simulation of space observations and signal component measurements, as well as atmospheric correction of real-time measurements of UST. Further improvement of the product aimed at perfection of its algorithmic basis and widening of functions is presumed.

References

1. V.V. Belov and S.V. Afonin, *From Basic Physics, Theory and Modeling to Topical Processing of Space Images* (Publishing House of IAO SB RAS, Tomsk, 2005), 266 pp.

2. S.V. Afonin and V.V. Belov, Atmos. Oceanic Opt. **18**, No. 12, 927–935 (2005).

3. A.S. Selivanov, Yu.M. Gektin, and F.V. Truskov, in: *Proc. of 3rd All-Russian Conf. on Aerospace Methods and GIS in Silvics and Forestry* (MSFU, Moscow, 2002), pp. 54–55.

4. F.X. Kneizys, E.P. Shettle, G.P. Anderson, L.W. Abreu, J.H. Chetwynd, J.E.A. Selby, S.A. Clough, and W.O. Gallery, User Guide to LOWTRAN-7. ARGL-TR-86-0177. ERP 1010 / Hansom AFB. MA 01731.

5. S.V. Afonin and V.V. Belov, Vychisl. Tekhnol. **8**, No. 11, 35–46 (2003).

6. S.V. Afonin, V.V. Belov, M.V. Engel, and A.M. Kokh, Atmos. Oceanic Opt. **18**, Nos. 1–2, 44–52 (2005).